








LETTER | JULY 17 2025

Sensing of ceftazidime antibiotics in human plasma through waveguide-enhanced Raman spectroscopy assisted by a mesoporous layer

Haolan Zhao ; Nuria Teigell Beneitez ; Himanshu Sekhar Jena ; Andre G. Skirtach ; Pascal Van Der Voort ; Roel Baets  



APL Photonics 10, 071302 (2025)

<https://doi.org/10.1063/5.0278252>



Articles You May Be Interested In

Isolation and purification of bacteriocin from *Escherichia coli* and study its synergistic effect with antibiotics and nanoparticles on pathogenic bacteria

AIP Conf. Proc. (December 2023)

Retraction: Antibiotic susceptibility pattern of *E. coli* causing urinary tract infection in pregnant women in Al-Najaf Province, Iraq

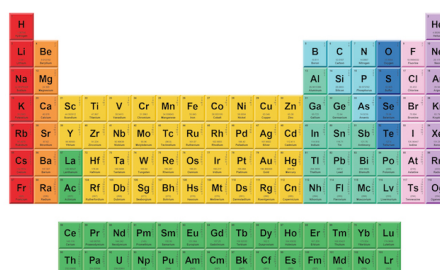
AIP Conf. Proc. (December 2023)

Multiple-loci number analyses of variable-number tandem repeat of molecular detection of *Staphylococcus aureus* isolates

AIP Conf. Proc. (March 2023)



Now Invent.™



American Elements
Opens a World of Possibilities

...Now Invent!

www.americanelements.com

© 2021-2024 American Elements is a U.S. Registered Trademark

Sensing of ceftazidime antibiotics in human plasma through waveguide-enhanced Raman spectroscopy assisted by a mesoporous layer

Cite as: APL Photon. 10, 071302 (2025); doi: 10.1063/5.0278252

Submitted: 29 April 2025 • Accepted: 28 June 2025 •

Published Online: 17 July 2025



Haolan Zhao,^{1,2,3}  Nuria Teigell Beneitez,^{1,2,3}  Himanshu Sekhar Jena,⁴  Andre G. Skirtach,⁵ 
Pascal Van Der Voort,⁴  and Roel Baets^{1,2,a)} 

AFFILIATIONS

¹ Photonics Research Group, INTEC, Ghent University-IMEC, 9052 Ghent, Belgium

² Center for Nano- and Biophotonics, Ghent University, 9052 Ghent, Belgium

³ Axithra, Zwijnaarde-Technologiepark 82/42, 9052 Ghent, Belgium

⁴ Department of Chemistry, Center for Ordered Materials, Organometallics and Catalysis (COMOC), Ghent University, Krijgslaan 281-S3, B-9000 Ghent, Belgium

⁵ Department of Biotechnology, Ghent University, 9000 Ghent, Belgium

^{a)} Author to whom correspondence should be addressed: Roel.Baets@ugent.be

ABSTRACT

We report, to the best of our knowledge, the first Raman sensor for antibiotics spiked in human plasma using silicon nitride waveguides functionalized with a mesoporous silica top-cladding. Leveraging waveguiding signal enhancement, chemical enrichment, and molecular sieving, we demonstrate detection of 1 mg/l ceftazidime in plasma within 2 min. Ceftazidime quantification is achieved in plasma over 0, 20, 40, and 60 mg/l, demonstrating its potential for clinical use. Requiring minimal sample preparation, this method has great potential for point-of-need monitoring for optimal antibiotic therapy.

© 2025 Author(s). All article content, except where otherwise noted, is licensed under a Creative Commons Attribution (CC BY) license (<https://creativecommons.org/licenses/by/4.0/>). <https://doi.org/10.1063/5.0278252>

Sepsis is one of the main causes for the morbidity and mortality in intensive care units (ICUs).¹ Caused by dysregulated immune response to infections, sepsis can lead to multiorgan damage and failure.² Early and adequate administration of antibiotics is considered a priority in the management of patients with sepsis.^{3,4} However, it is challenging to maintain optimal antibiotic exposure in ICU patients due to their rapid and sometimes extreme physiological changes. Therefore, the primary focus for success of treatment is timely dose adjustment of antibiotic therapy.⁵

Current methodologies for quantifying β -lactam antibiotics in plasma predominantly rely on chromatographic techniques, which necessitate extensive sample pretreatment and the involvement of trained personnel. These requirements contribute to prolonged turnaround times, sometimes up to days,^{6,7} thereby limiting the clinical utility of the results. This delay underscores the pressing need for a point-of-need analytical platform capable of delivering rapid and

accurate antibiotic quantification directly from blood with minimal sample preparation.

Raman spectroscopy is an ideal candidate for this objective since it is capable of label-free molecular fingerprinting. It probes the molecular vibrations by recording the spectrum of laser photons scattered inelastically by the analytes. The spectrum allows the quantification of antibiotics directly from a complicated matrix with minimal sample preparation.⁸ In contrast to infrared spectroscopy, Raman does not suffer from a strong water background, making it suitable for aqueous biological samples. Unfortunately, Raman scattering is an extremely inefficient process where typically only one out of 10^6 – 10^8 incident photons are Raman scattered.⁹ Utilizing the tremendous electromagnetic field enhancement in the vicinity of metallic nanostructures, surface-enhanced Raman spectroscopy (SERS) has been successfully demonstrated for the quantification of therapeutic drugs.^{10–13} However, SERS is very sensitive to the

variability of the metallic structures,¹⁴ and its capability in real clinical settings has yet to be proved.

An emerging promising approach to enhance the signal is to tightly confine both the optical excitation and the analyte within hollow fibers, where a large ensemble of molecules can participate in Raman scattering and contribute to the signal. Sensitive antibiotic sensing in μM concentration range has been demonstrated with hollow-core fibers filled with analytes.^{15,16} However, users will have to fill the fiber core with liquid sample prior to sensing, which is challenging for point-of-need applications.

More recently, waveguide-enhanced Raman spectroscopy (WERS) using single-mode silicon nitride (SiN) waveguides on a chip has gained popularity.^{17–21} In this approach, the fluid serves as the cladding for a functionalized waveguide, enabling excitation of analyte molecules by the guided optical mode. These molecules subsequently scatter light into both the forward- and backward-propagating guided modes. The photonic integrated waveguides avoid the challenges in filling the fibers with sample liquids. Silicon nitride, with its relatively high refractive index, when combined with slot waveguides, enables one to enhance the confinement of the optical field within the slot region, thereby significantly improving the Raman efficiency.²² Furthermore, the photonic integrated waveguides also allow integration with solid-phase extraction media to trap and concentrate organic analytes from the matrix prior to Raman interaction.^{23,24} In particular, the waveguides can be coated with a sorbent layer that locally pre-concentrates analytes based on their general chemical properties, such as hydrophilicity and lipophilicity. The Raman signal from analytes within the sorbent cladding is excited and collected via the evanescent field of the guided optical mode. This signal is then coupled back into the waveguide and propagates in a guided mode. Raman scattering occurs in both the co-propagating and counter-propagating directions relative to the excitation laser, allowing spectral analysis to be performed by collecting light from either end of the waveguide.^{17,18} It is worth noting that the co-propagated Raman signal exhibits an optimal waveguide length, beyond which the signal begins to decline. In contrast, the counter-propagating Raman signal always increases with waveguide length. Therefore, the counter-propagating configuration

is preferred in this work. Leveraging both analyte enrichment and waveguiding effect, ultrasensitive gas and liquid analyte detection down to ppm-to-ppb-levels has been demonstrated.^{21,23} However, in previously reported studies, analytes were typically prepared in simple buffer solutions free from interfering components. This raises an important question regarding the applicability of the functionalized waveguide approach in more complex matrices, where a diverse array of co-existing molecules will be present and potentially interfere with analyte detection.

In this work, we investigate the clinical applicability of functionalized SiN waveguides for the quantification of antibiotics in human plasma. We report the WERS detection of ceftazidime, a model antibiotic, at therapeutically relevant concentrations ranging from 8 to 80 mg/l. Furthermore, we demonstrate a clear concentration-dependent Raman response, underscoring the potential of functionalized waveguides as a viable platform for point-of-care antibiotic quantification.

The photonic chip is fabricated by IMEC on the BioPIX platform.²⁵ A layer of 300-nm-thick SiN layer is deposited on top of a 3.3- μm -thick buried oxide via plasma-enhanced chemical vapor deposition (PECVD). The waveguides are patterned via deep-UV photolithography and reactive ion etching. They have a nominal cross section of $w \times h = 600 \times 300 \text{ nm}^2$ with a slot of 150 nm. The waveguides are terminated with 3- μm -wide strip waveguides for edge coupling at both ends. The waveguides are covered with a layer of 2- μm -thick top oxide. Part of the top oxide is later removed to expose an 8-mm-long and 0.5-mm-wide section for sensing. Such slot waveguides are employed in this measurement due to their better Raman performance.^{18,19,26} A mesoporous silica coating is then introduced and functionalized on top of the slot waveguide section with the technique explained in detail in Refs. 21 and 27–29. It is noteworthy that the pore size of the coating is adjusted to 4 nm, as confirmed by *in situ* measurements on chips fabricated in the same batch for this work,³⁰ to make sure that large interfering molecules, e.g., proteins and cholesterol, are rejected from the coating while the antibiotics can diffuse into it. The cross section of the sensing waveguide is shown in Fig. 1(b). The coating functions as a molecular sieve, effectively limiting interference from other

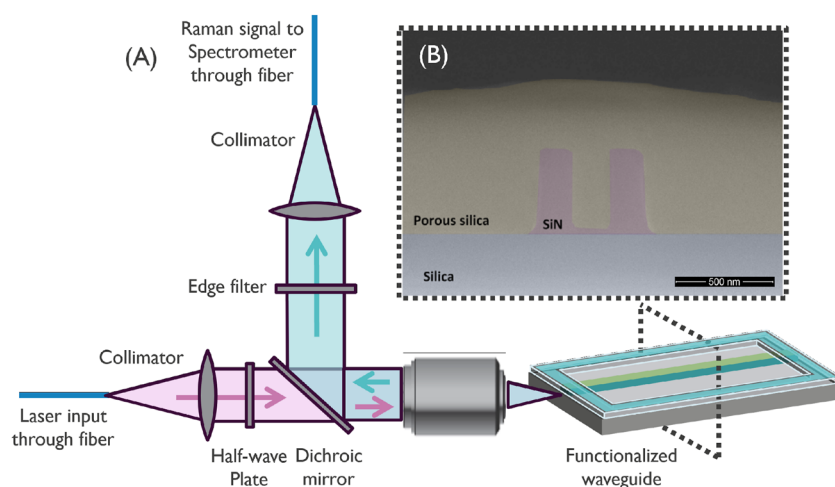


FIG. 1. (a) Schematic representation of the Raman microscopy setup used for the characterization of functionalized waveguides. The arrows indicate the direction of light propagation within the system. (b) SEM cross section of the functionalized slot waveguide. Different materials are marked in pseudo-color.

endogenous components. The effective index of the sorbent is 1.39 when filled with plasma, as calculated from Bruggeman effective medium approximation.³¹

Experiments are performed with a confocal Raman microscope (WITec Alpha 300 R) with a 785 nm pump laser (Toptica XTRA II), as shown in Fig. 1(a). The polarization of the pump beam is controlled using a half-wave plate to excite the fundamental TE mode of the slotted waveguide, and the pump power before the objective is set to 40 mW. The pump laser is coupled to the chip via an objective (Olympus 100 \times , NA0.9), and the backward-propagating Raman signal is captured via the same objective. The optical chip is held by using a homemade liquid cell, which holds 0.7 ml plasma sample for sensing. The coupling loss is measured to be 7.5 dB/facet. The collected Raman signal is sent to a spectrometer (UHTS400 with Andor iDus 401 camera cooled to -60°C) for analysis. The integration time of each measurement is 0.5 s, and the spectra are averaged over 20 measurements.

Ceftazidime antibiotics used for experiments are purchased from Fresenius Kabi. This antibiotic is widely used in clinical settings and is characterized by a short elimination half-life of approximately 1–2 h.³² Consequently, rapid point-of-need monitoring is essential to support timely and effective therapeutic decisions. In this study, pooled human plasma (Biowest, Product S4180) was used as the biological matrix. Following dissolution of the antibiotic powder in plasma, the solution was acidified with hydrochloric acid to a pH below 5 to maximize chemical enrichment within the waveguide coating.³³

Figure 2 presents the representative Raman spectra acquired from the functionalized waveguide for water (black dotted curve), blank plasma (orange curve), and ceftazidime-spiked plasma (blue curve). To assess the influence of the surface coating, the Raman spectrum obtained from an uncoated SiN waveguide is also shown (green dotted curve).

An additional Raman peak at 1600 cm^{-1} is observed superimposed on the SiN waveguide background, consistent with previous reports.^{17,23} This feature is attributed to the functional groups in the mesoporous coating and proves advantageous for quantitative analysis. Since antibiotic enrichment is expected to correlate with the density of functional groups within the coating, the ratio of the antibiotic signal to the 1600 cm^{-1} peak should remain stable. This normalization strategy enhances robustness against potential fabrication-induced variability in the waveguide platform.

Furthermore, the spectral similarity observed between blank plasma and water suggests a molecular sieving effect imparted by the sorbent layer.

Upon exposure to ceftazidime-spiked plasma, distinct Raman features emerge at 1029, 1407, and 1451 cm^{-1} . Peaks at 1586 and 1640 cm^{-1} are also detected, although they are spectrally close to the 1600 cm^{-1} peak.

The inset of Fig. 2 provides a detailed view of the ceftazidime signal in the $1500\text{--}1700\text{ cm}^{-1}$ spectral region. Background contributions were removed using polynomial fitting. The resulting waveguide Raman signal (black curve) was then deconvoluted to isolate the ceftazidime-specific peaks at 1586 and 1640 cm^{-1} (solid blue curve) through peak fitting. The combined fit of these two peaks with the 1600 cm^{-1} background feature (dotted blue curve) accurately reconstructs the measured spectrum (red curve). Notably, the 1600 cm^{-1} peak, originating from the mesoporous coating, is employed as an internal reference to normalize spectral variations, thereby enhancing the reliability of ceftazidime quantification.

To confirm that the observed Raman bands at Fig. 2 are indeed arising from ceftazidime, we compare the WERS ceftazidime signal to the free-space reference in Fig. 3. The free-space measurement is carried out with a concentrated ceftazidime solution at 10 000 mg/l, because the Raman signal from 200 mg/l of ceftazidime cannot be readily separated from the solution background.

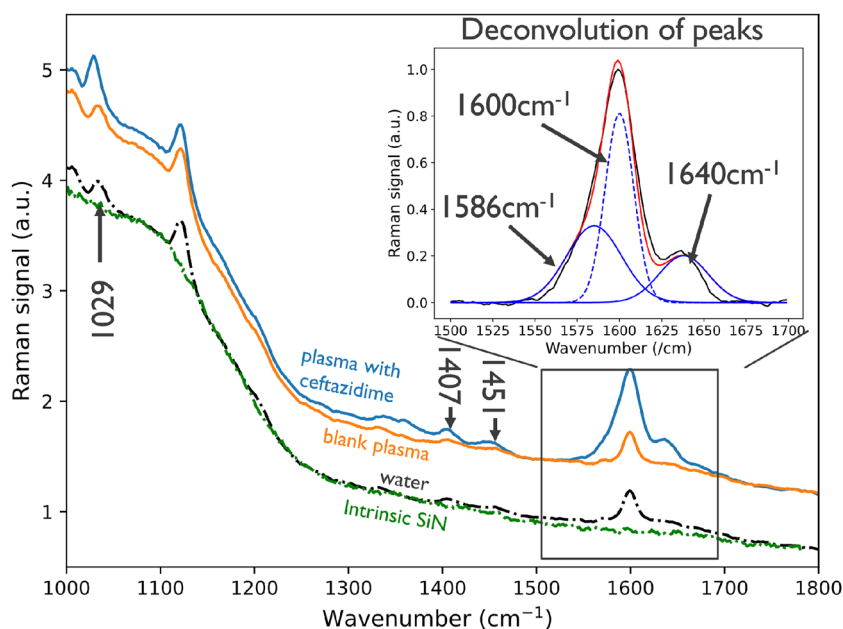


FIG. 2. Raman spectra acquired from functionalized waveguides in water (black dotted line), blank plasma (orange solid line), and ceftazidime-spiked plasma (blue solid line), shown relative to the intrinsic background of uncoated SiN waveguides (green dotted line). Spectra involving plasma have been vertically offset for clarity. The inset illustrates the deconvolution of the signal into its constituent ceftazidime peaks at 1586 and 1640 cm^{-1} (blue solid lines) and coating peak at 1600 cm^{-1} (dashed blue curve). The combination of these three peaks (red line) closely reconstructs the measured spectrum (black line).

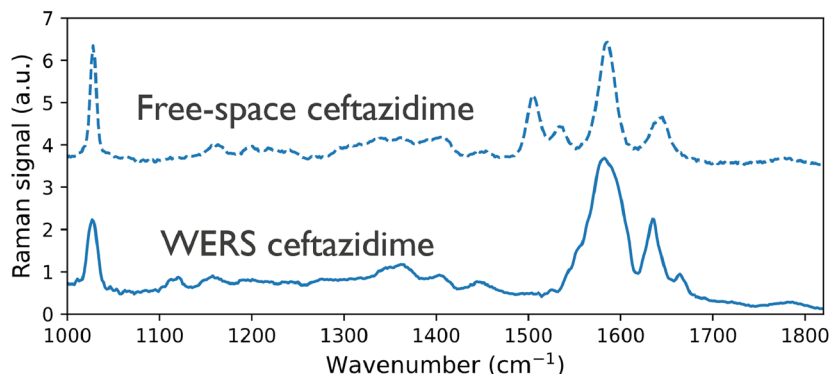


FIG. 3. Background-subtracted WERS spectra of ceftazidime at 200 mg/l are compared with a reference free-space spectrum acquired at 10 000 mg/l. The majority of ceftazidime spectral features observed in the free-space reference are present in the waveguide measurements.

Most of the signature bands at 1029, 1407, 1451, 1586, and 1640 cm^{-1} , from free-space reference ceftazidime spectra, can be observed in the waveguide measurements. It indicates that the deconvolved WERS signal is indeed induced by ceftazidime. However, some bands, most notably the ones at 1505 and 1535 cm^{-1} , are missing from the WERS result. This is probably due to the change of the ceftazidime chemical bond when adsorbed by the silica framework, which has been observed with other molecules.^{34,35}

Notably, when measuring a concentration of 60 mg/L of antibiotics using both WERS and free-space configurations, under identical laser power and integration time, the waveguide-based signal will be ~ 110 times stronger than that of the free-space setup, despite the 7.5 dB/facet waveguide coupling loss. This substantial enhancement underscores the synergy provided by the waveguide enhancement and the sorbent for relevant antibiotic concentration range.

To evaluate whether the functionalized waveguide is capable of quantifying ceftazidime over the relevant concentration range of 0–80 mg/l, a total of 12 spiked plasma samples are prepared,

each with 0, 20, 40, or 60 mg/l ceftazidime (3 repeats each). For each sample, its Raman response is recorded with a new chip to avoid the carryover effect. In each measurement, the chip is first exposed to water to record the Raman background of the chip for peak deconvolution. For each plasma result, we first subtract the background using the polynomial fitting, then deconvolve the ceftazidime signal from waveguides, and eventually normalize the ceftazidime spectrum by the 1600 cm^{-1} waveguide background peak. The average ceftazidime Raman spectrum for each concentration is shown in Fig. 4(a). First of all, it can be noticed that blank plasma (0 mg/l ceftazidime) exhibits no discernible peaks, highlighting that the mesoporous coating effectively repels interfering molecules from the waveguide. For plasma samples containing ceftazidime, their Raman spectra exhibit two signature peaks at 1586 and 1639 cm^{-1} .

The peak area for the 1586 cm^{-1} band is employed to construct the calibration curve as shown in Fig. 4(b). The calibration curve has a non-zero intercept, which indicates a non-perfect background subtraction. Regardless, it is interesting to observe a good

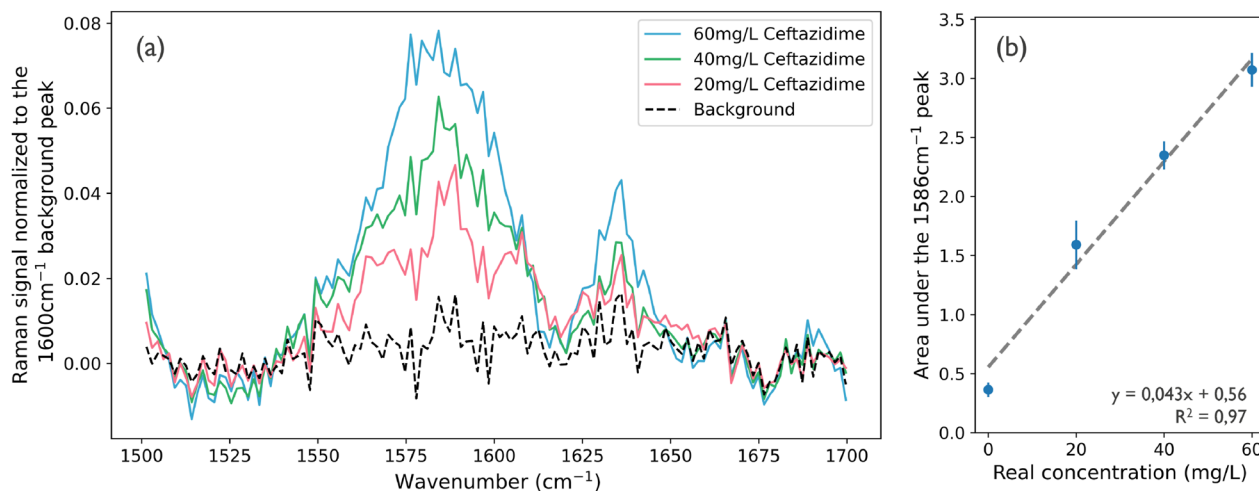


FIG. 4. (a) Deconvolved ceftazidime Raman spectrum in plasma at various concentrations. The ceftazidime peaks are normalized against the 1600 cm^{-1} waveguide background. (b) The area under the 1586 cm^{-1} peak is employed for quantification, and the error bar corresponds to quantification variations from different chips.

degree of linearity between the 1586 cm^{-1} peak area and the ceftazidime concentration. The adsorption of ceftazidime in the coating is typically governed by the Langmuir or Freundlich model.³⁶ Both models predict that ceftazidime adsorption within the coating approaches saturation beyond a specific concentration threshold. The near-linear response in Fig. 4(b) observed across the tested range suggests that the coating remains largely below saturation, thereby confirming the functionalized waveguide's capability to operate reliably over clinically relevant concentration levels.

The functionalized SiN waveguides demonstrate good reproducibility in quantitative measurements. The relative standard deviations (RSDs) for ceftazidime concentrations of 20, 40, and 60 mg/l are 17.0%, 4.5%, and 4.6%, respectively. These values are comparable to the acceptance criteria for current chromatographic assays, which typically require RSDs below 15% for bioanalytical methods.³⁷ These findings highlight the potential of functionalized waveguides as a viable platform for TDM applications.

To explore the detection limit of the functionalized waveguides, we expose the waveguides to 1 mg/l of ceftazidime in plasma. The normalized and background-subtracted Raman peak before and after ceftazidime exposure is shown in Fig. 5. The variation from three waveguides from the same chip, all exposed to the same plasma, is shown as the shaded area. Although it is not possible to measure the same plasma sample with and without 1 mg/l ceftazidime, the result still indicates the intrinsic capability of our method. It is noteworthy that these spectra are recorded with a 2-min measurement time and smoothed by using a 9-point moving average filter.

It is noteworthy that the sensor exhibits a very short measurement time, which is essential for effective point-of-need monitoring. In the current demonstration, chip alignment following plasma injection into the liquid cell requires $\sim 1\text{--}2$ min. By this time, the Raman signal corresponding to the antibiotics has already stabilized, indicating complete diffusion into the coating and the establishment of equilibrium. Consequently, the total turnaround

time from plasma introduction to result acquisition does not exceed 5 min, representing a substantial improvement over current clinical practices.⁶

In this Letter, we showed that WERS produced with functionalized SiN waveguides can be a candidate for point-of-need antibiotic monitoring. The antibiotic signal can be reliably probed by combining (1) chemical enrichment of antibiotics at the mesoporous top-cladding, (2) exciting and collecting Raman signal along the entire waveguide, and (3) repelling interfering components from plasma with the small pore size.

Using the functionalized waveguide platform, we investigated β -lactam antibiotics spiked into human plasma. Distinct Raman spectral features were consistently observed at clinically relevant concentrations, indicating the sensor's broad applicability across multiple antibiotic compounds. For ceftazidime, a reliable and reproducible calibration curve was established using its characteristic Raman band at 1586 cm^{-1} , with plasma concentrations of 0, 20, 40, and 60 mg/l. Although the mesoporous layer introduces additional Raman background, it does not hinder quantification. In fact, the 1600 cm^{-1} peak originating from the coating serves as an effective internal standard for normalization, mitigating systematic variations. These attributes, combined with a rapid turnaround time of a few minutes and random-access sample handling, position WERS with functionalized waveguides as a compelling candidate for point-of-need antibiotic monitoring. We envision the final solution to be a PIC embedded within a single-use consumable cartridge, enabling automated and minimal sample preparation. The user would simply insert the cartridge into a readout device, which then generates the Raman signal for antibiotic quantification.

The authors acknowledge ERC Advanced Grant InSpectra (Grant No. 267853), ERC Proof-of-Concept MiraSpec (Grant No. 780718), FWO (Grant No. 1002620N), and Methusalem Grant "Smart Photonic Chips" of R. Baets from Flemish Government.

AUTHOR DECLARATIONS

Conflict of Interest

H.Z. and N.T.B. are now employees of or consultants for Axithra and may have stock or stock options in the company. H.S.J., A.G.S., P.V.D.V., and R.B. declare no conflict of interest.

Author Contributions

Haolan Zhao: Investigation (equal); Writing – original draft (equal); Writing – review & editing (equal). **Nuria Teigell Beneitez:** Investigation (supporting); Writing – review & editing (equal). **Himanshu Sekhar Jena:** Investigation (supporting); Writing – review & editing (equal). **Andre G. Skirtach:** Writing – review & editing (equal). **Pascal Van Der Voort:** Conceptualization (equal); Writing – review & editing (equal). **Roel Baets:** Supervision (equal); Writing – review & editing (equal).

DATA AVAILABILITY

The data that support the findings of this study are available from the corresponding author upon reasonable request.

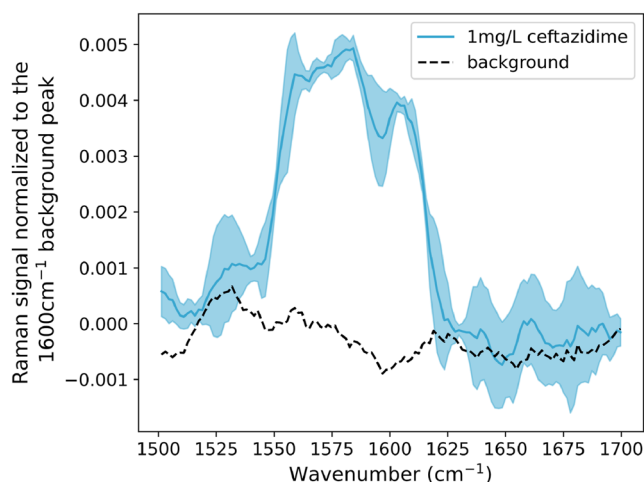


FIG. 5. Deconvoluted 1 mg/l ceftazidime signal from plasma. The variation of the 1 mg/l Raman peak shown as the shaded area is obtained from three waveguides from the same photonic chip, all exposed to the same spiked plasma.

REFERENCES

- ¹M. Wang, L. Jiang, B. Zhu, W. Li, B. Du, Y. Kang, L. Weng, T. Qin, X. Ma, D. Zhu *et al.*, "The prevalence, risk factors, and outcomes of sepsis in critically ill patients in China: A multicenter prospective cohort study," *Front. Med.* **7**, 593808 (2020).
- ²S. Hagel, S. Fiedler, A. Hohn, A. Brinkmann, O. R. Frey, H. Hoyer, P. Schlattmann, M. Kiehnopf, J. A. Roberts, M. W. Pletz, F. Bloos, S. Angermair, H. Bracht, E. Barth, S. Kluge, A. Nierhaus, J. Motsch, T. Brenner, T. Annecke, F. Bach, M. Weigand, M. Schappacher, A. V. Ameln-Mayerhofer, G. Michels, A. Roehr, T. Fuchs, S. Eichner, C. Köng, N. Pinder, C. Müller, M. Petersen, G. Steinbach, D. Jarczak, D. Weisman, M. Kurlbaum, and A. Braune, "Therapeutic drug monitoring-based dose optimisation of piperacillin/tazobactam to improve outcome in patients with sepsis (TARGET): A prospective, multi-centre, randomised controlled trial," *Trials* **20**, 330 (2019).
- ³R. Guilhaumou, S. Benaboud, Y. Bennis, C. Dahyot-Fizelier, E. Dailly, P. Gandia, S. Goutelle, S. Lefeuvre, N. Mongardon, C. Roger, J. Scala-Bertola, F. Lemaitre, and M. Garnier, "Optimization of the treatment with beta-lactam antibiotics in critically ill patients—guidelines from the french society of pharmacology and therapeutics (société française de pharmacologie et thérapeutique—SFPT) and the french society of anaesthesia and intensive care medicine (société française d'anesthésie et réanimation—SFAR)," *Crit. Care* **23**, 104 (2019).
- ⁴P. W. Smith, F. Zuccotto, R. H. Bates, M. S. Martinez-Martinez, K. D. Read, C. Peet, and O. Epemolu, "Pharmacokinetics of β -lactam antibiotics: Clues from the past to help discover long-acting oral drugs in the future," *ACS Infect. Dis.* **4**, 1439–1447 (2018).
- ⁵A. Tabah, J. D. Waele, J. Lipman, J. R. Zahar, M. O. Cotta, G. Barton, J.-F. Timsit, and J. A. Roberts, "The ADMIN-ICU survey: A survey on antimicrobial dosing and monitoring in ICUs," *J. Antimicrob. Chemother.* **70**, 2671–2677 (2015).
- ⁶M. Shipkova and H. Jamoussi, "Therapeutic drug monitoring of antibiotic drugs: The role of the clinical laboratory," *Ther. Drug Monit.* **44**, 32–49 (2022).
- ⁷M. Carlier, V. Stove, S. C. Wallis, J. J. De Waele, A. G. Verstraete, J. Lipman, and J. A. Roberts, "Assays for therapeutic drug monitoring of β -lactam antibiotics: A structured review," *Int. J. Antimicrob. Agents* **46**, 367–375 (2015).
- ⁸J. Y. Qu and L. Shao, "Near-infrared Raman instrument for rapid and quantitative measurements of clinically important analytes," *Rev. Sci. Instrum.* **72**, 2717–2723 (2001).
- ⁹E. Smith and G. Dent, *Modern Raman Spectroscopy: A Practical Approach* (John Wiley & Sons, 2019).
- ¹⁰C. Liu, C. Franceschini, S. Weber, T. Dib, P. Liu, L. Wu, E. Farnesi, W.-s. Zhang, V. Sivakov, P. B. Lupp, J. Popp, and D. Cialla-May, "SERS-based detection of the antibiotic ceftriaxone in spiked fresh plasma and microdialysate matrix by using silver-functionalized silicon nanowire substrates," *Talanta* **271**, 125697 (2024).
- ¹¹X. Wang, J. Zeng, Q. Sun, J. Yang, Y. Xiao, Z. Zhu, B. Yan, and Y. Li, "An effective method towards label-free detection of antibiotics by surface-enhanced Raman spectroscopy in human serum," *Sens. Actuators B: Chem.* **343**, 130084 (2021).
- ¹²N. E. Markina, A. V. Markin, and D. Cialla-May, "Cyclodextrin-assisted SERS determination of fluoroquinolone antibiotics in urine and blood plasma," *Talanta* **254**, 124083 (2023).
- ¹³Y. Göksel, E. Dumont, R. Slipets, S. T. Rajendran, S. Sarikaya, L. H. E. Thammurup, K. Schmiegelow, T. Rindzevicius, K. Zor, and A. Boisen, "Methotrexate detection in serum at clinically relevant levels with electrochemically assisted SERS on a benchtop, custom built Raman spectrometer," *ACS Sens.* **7**, 2358–2369 (2022).
- ¹⁴A. Y. F. Mahmoud, A. Teixeira, M. Aranda, M. S. Relvas, S. Quintero, M. Sousa-Silva, A. Chicharo, M. Chen, M. Hashemi, J. B. King, J. W. Tunnell, C. Morasso, F. Piccotti, F. Corsi, M. Henriksen-Lacey, D. J. de Aberasturi, D. Méndez-Merino, A. Rodríguez-Patón, S. Abalde-Cela, and L. Diéguez, "Will data analytics revolution finally bring SERS to the clinic?," *TrAC, Trends Anal. Chem.* **169**, 117311 (2023).
- ¹⁵D. Yan, T. Frosch, J. Kobelke, J. Bierlich, J. Popp, M. W. Pletz, and T. Frosch, "Fiber-enhanced Raman sensing of cefuroxime in human urine," *Anal. Chem.* **90**, 13243–13248 (2018).
- ¹⁶D. Yan, J. Popp, M. W. Pletz, and T. Frosch, "Fiber enhanced Raman sensing of levofloxacin by PCF bandgap-shifting into the visible range," *Anal. Methods* **10**, 586–592 (2018).
- ¹⁷A. Dhakal, A. Z. Subramanian, P. Wuytens, F. Peyskens, N. L. Thomas, and R. Baets, "Evanescent excitation and collection of spontaneous Raman spectra using silicon nitride nanophotonic waveguides," *Opt. Lett.* **39**, 4025–4028 (2014).
- ¹⁸A. Dhakal, A. Raza, F. Peyskens, A. Z. Subramanian, S. Clemmen, N. Le Thomas, and R. Baets, "Efficiency of evanescent excitation and collection of spontaneous Raman scattering near high index contrast channel waveguides," *Opt. Express* **23**, 27391–27404 (2015).
- ¹⁹D. M. Kita, J. Michon, S. G. Johnson, and J. Hu, "Are slot and sub-wavelength grating waveguides better than strip waveguides for sensing?," *Optica* **5**, 1046 (2018).
- ²⁰D. M. Kita, J. Michon, and J. Hu, "A packaged, fiber-coupled waveguide-enhanced Raman spectroscopic sensor," *Opt. Express* **28**, 14963 (2020).
- ²¹Z. Liu, H. Zhao, B. Baumgartner, B. Lendl, A. Stassen, A. Skirtach, N. L. Thomas, and R. Baets, "Ultra-sensitive slot-waveguide-enhanced Raman spectroscopy for aqueous solutions of non-polar compounds using a functionalized silicon nitride photonic integrated circuit," *Opt. Lett.* **46**, 1153 (2021).
- ²²A. Dhakal, "Nanophotonic waveguide enhanced Raman spectroscopy," Ph.D. thesis, Ghent University, 2016.
- ²³S. A. Holmstrom, T. H. Stievater, D. A. Kozak, M. W. Pruessner, N. Tyn-dall, W. S. Rabinovich, R. Andrew McGill, and J. B. Khurgin, "Trace gas Raman spectroscopy using functionalized waveguides," *Optica* **3**, 891–896 (2016).
- ²⁴K. J. Ewing, G. Nau, T. Bilodeau, D. M. Dagenais, F. Bucholtz, and I. D. Aggarwal, "Monitoring the absorption of organic vapors to a solid phase extraction medium applications to detection of trace volatile organic compounds by integration of solid phase absorbents with fiber optic Raman spectroscopy," *Anal. Chim. Acta* **340**, 227–232 (1997).
- ²⁵A. Z. Subramanian, E. Ryckeboer, A. Dhakal, F. Peyskens, A. Malik, B. Kuyken, H. Zhao, S. Pathak, A. Ruocco, A. De Groote, P. Wuytens, D. Martens, F. Leo, W. Xie, U. D. Dave, M. Muneeb, P. Van Dorpe, J. Van Campenhout, W. Bogaerts, P. Bienstman, N. Le Thomas, D. Van Thourhout, Z. Hens, G. Roelkens, and R. Baets, "Silicon and silicon nitride photonic circuits for spectroscopic sensing on-a-chip [invited]," *Photonics Res.* **3**, B47 (2015).
- ²⁶H. Zhao, B. Baumgartner, A. Raza, A. Skirtach, B. Lendl, and R. Baets, "Multiplex volatile organic compound Raman sensing with nanophotonic slot waveguides functionalized with a mesoporous enrichment layer," *Opt. Lett.* **45**, 447–450 (2020).
- ²⁷B. Baumgartner, J. Hayden, A. Schwaighofer, and B. Lendl, "In situ ir spectroscopy of mesoporous silica films for monitoring adsorption processes and trace analysis," *ACS Appl. Nano Mater.* **1**, 7083–7091 (2018).
- ²⁸B. Baumgartner, J. Hayden, J. Loizillon, S. Steinbacher, D. Grosso, and B. Lendl, "Pore size-dependent structure of confined water in mesoporous silica films from water adsorption/desorption using ATR–FTIR spectroscopy," *Langmuir* **35**, 11986–11994 (2019).
- ²⁹B. Baumgartner, "Mid-infrared spectroscopy and porous oxides: From trace analysis to interactions at surfaces," Ph.D. thesis, Technische Universität Wien, 2019.
- ³⁰J. Dendooven, K. Devloo-Casier, E. Levrau, R. Van Hove, S. Pulinthanathu Sree, M. R. Baklanov, J. A. Martens, and C. Detavernier, "In situ monitoring of atomic layer deposition in nanoporous thin films using ellipsometric porosimetry," *Langmuir* **28**, 3852–3859 (2012).
- ³¹M. Sela and C. Haspel, "Predicting the refractive index of amorphous materials using the Bruggeman effective medium approximation," *Appl. Opt.* **59**, 8822–8827 (2020).
- ³²S. R. Norrby, L. Å. Burman, H. Linderholm, and B. Trollfors, "Ceftazidime: Pharmacokinetics in patients and effects on the renal function," *J. Antimicrob. Chemother.* **10**, 199–206 (1982).
- ³³P. Colin, L. De Bock, H. T'Jolyn, K. Boussery, and J. Van Bocxlaer, "Development and validation of a fast and uniform approach to quantify β -lactam antibiotics in human plasma by solid phase extraction-liquid chromatography–electrospray-tandem mass spectrometry," *Talanta* **103**, 285–293 (2013).

³⁴K. Y. Foo and B. H. Hameed, “Insights into the modeling of adsorption isotherm systems,” *Chem. Eng. J.* **156**, 2–10 (2010).

³⁵K. Jeong, A. Arami-Niya, X. Yang, G. Xiao, G. Lipinski, Z. M. Aman, E. F. May, M. Richter, and P. L. Stanwix, “Direct characterization of gas adsorption and phase transition of a metal organic framework using in-situ Raman spectroscopy,” *Chem. Eng. J.* **473**, 145240 (2023).

³⁶Q.-Z. Zhai, Y. Dong, H. Liu, and Q.-S. Wang, “Adsorption of methylene blue onto nano SBA-15 mesoporous material from aqueous media: Kinetics, isotherms and thermodynamic studies,” *Desalin. Water Treat.* **158**, 330 (2019).

³⁷EMA/CHMP/ICH/172948/2019, ICH guideline M10 on bioanalytical method validation, Guidelines, Committee for Medicinal Products for Human Use, 2023.